

Engineering Notes

Multiple-Revolution Solutions of the Transverse-Eccentricity-Based Lambert Problem

Quan He,* Jian Li,† and Chao Han‡

Beijing University of Aeronautics and Astronautics,
100191 Beijing, People's Republic of China

DOI: 10.2514/1.45041

I. Introduction

THIS Engineering Note follows a previous paper in which Avanzini [1] presented a transverse-eccentricity-vector-based algorithm to solve the classical Lambert problem: that is, the determination of a transfer orbit having a specified flight time and connecting two position vectors [2]. In Avanzini's [1] paper, the eccentricity vector of the transfer orbit can be decomposed into a constant component parallel to the chord connecting the two points and a variable transverse component in the direction perpendicular to it on the orbit plane. Given the two fixed position vectors, the transfer time can be expressed as a function of the transverse eccentricity e_T . Compared with the elegant Battin's method, the derivation of this simple Lambert algorithm seems to be considerably less demanding from the mathematical standpoint and physically more intuitive [1]. However, with the only consideration of direct-transfer arcs, neither the explicit expression of the derivative of the transfer time with respect to the transverse eccentricity nor the multiple-revolution solutions based on the novel method were given in [1].

The multiple-revolution Lambert's problem has been being discussed since the 1980s [3]. After the 1990s, mainly based on Ochoa's works [4], many experts studied the multiple-revolution using the classical Lagrange formulation for an elliptic transfer orbit, where the transfer time was expressed as a function of semimajor axis. Prussing [5] developed a minimum-fuel multiple-revolution algorithm for an elliptic orbit to determine all the possible transfer trajectories, based on the classical Lagrange formulation. Also based on this formulation, Shen and Tsotras [6] presented a minimum- ΔV , fixed-time, two-impulse transfer algorithm between two coplanar circular orbits. In Shen and Tsotras's algorithm, only two of the multiple-revolution solutions need to be calculated and compared to obtain the minimum-cost transfer orbit. In addition to the Lagrange formulation method, it is also possible to use universal variables to solve the multiple-revolution problem [7]. Han and Xie [8] also presented a homologous algorithm to obtain the multiple-revolution solutions using these variables. In [8], the transfer time was written as a function of universal variable z , for which the value is limited to the boundary

$$4N^2\pi^2 < z < 4(N+1)^2\pi^2$$

for a given number of revolutions N . Then all the solutions for z were calculated and compared to determine a minimum-fuel transfer trajectory.

In this Note, the analysis of [1] is extended to the case of multiple revolutions. First, Avanzini's transverse-eccentricity-based Lambert formulation is generalized to the multiple-revolution Lambert problem. Given two fixed points in space, the multiple-revolution transfer time can be expressed as a function of the transverse-eccentricity component e_T and the number of admissible revolutions N , and then the corresponding derivative of the transfer time relative to the transverse eccentricity is derived. Moreover, the transverse-eccentricity-based numerical procedure to obtain the solutions of the multiple-revolution Lambert's problem is proposed, and numerical simulations are carried out in the end to validate it.

II. Multiple-Revolution Lambert's Problem

Figure 1 shows the basic orbital geometry of the classical Lambert problem. In Fig. 1, F is the center of the gravitation, P_1 and P_2 are the given initial and final positions in space, c is the chord length between the two points, and the radius vectors \mathbf{r}_1 and \mathbf{r}_2 locate the points P_1 and P_2 with respect to the focus F . The angle $\Delta\theta$ between radius vectors is the transfer angle, and \mathbf{e} is the eccentricity vector of the orbit.

As described in [1], the component of the eccentricity vector projecting onto the chord P_1P_2 is constant and can be expressed as

$$e_f = \mathbf{e} \cdot \mathbf{i}_c = \mathbf{e} \cdot (\mathbf{r}_2 - \mathbf{r}_1)/c = (r_1 - r_2)/c \quad (1)$$

where \mathbf{i}_c is the chord unit vector, $c = \|\mathbf{r}_2 - \mathbf{r}_1\|$, and r_1 and r_2 are the magnitudes of the corresponding radius vectors. The component of the eccentricity vector perpendicular to the chord is defined as the transverse eccentricity e_T . Thus, the eccentricity vector of the transfer orbit passing through P_1 and P_2 can be decomposed into a constant component parallel to the chord e_f and a variable transverse component perpendicular to the chord e_T , then the vector can be written as

$$\mathbf{e} = e_f \mathbf{i}_c + e_T \mathbf{i}_p \quad (2)$$

where \mathbf{i}_p is the unit vector lying in the orbit plane and perpendicular to the chord direction, as shown in Fig. 1.

One gets the minimum eccentricity admissible transfer orbit when the transverse eccentricity is equal to zero. Battin [3] defined this minimum eccentricity orbit as the fundamental ellipse, for which the eccentricity, semimajor axis, and semilatus rectum are given by

$$\begin{cases} e_f = (r_1 - r_2)/c \\ a_f = (r_1 + r_2)/2 \\ p_f = a_f(1 - e_f^2) \end{cases} \quad (3)$$

where the subscript f denotes the fundamental ellipse solution.

As discussed in [1], the semilatus rectum of a generic transfer orbit can be expressed as a function of the transverse eccentricity as follows:

$$p(e_T) = p_f - e_T \frac{r_1 r_2}{c} \sin(\Delta\theta) \quad (4)$$

The semimajor axis and orbit period can be expressed as

$$\begin{cases} a(e_T) = p(e_T)/(1 - e_f^2 - e_T^2) \\ T(e_T) = 2\pi\sqrt{a^3/\mu} \end{cases} \quad (5)$$

where μ is the gravitational constant.

Received 20 April 2009; revision received 14 October 2009; accepted for publication 14 October 2009. Copyright © 2009 by He Quan, Li Jian, and Han Chao. Published by the American Institute of Aeronautics and Astronautics, Inc., with permission. Copies of this paper may be made for personal or internal use, on condition that the copier pay the \$10.00 per-copy fee to the Copyright Clearance Center, Inc., 222 Rosewood Drive, Danvers, MA 01923; include the code 0731-5090/10 and \$10.00 in correspondence with the CCC.

*Ph.D. Candidate, School of Astronautics; hequanhq@sa.buaa.edu.cn. Student Member AIAA.

†Ph.D. Candidate, School of Astronautics; lijian@sa.buaa.edu.cn.

‡Professor, School of Astronautics; hanchao@buaa.edu.cn.

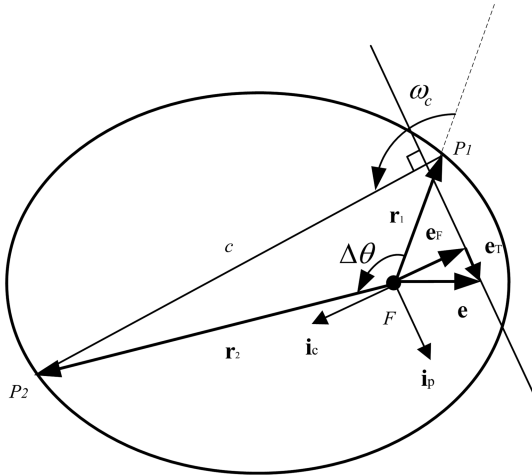


Fig. 1 Transfer orbit geometry of the Lambert problem.

The true anomalies of P_1 and P_2 are given by

$$\begin{cases} \theta_1 = -\tan^{-1}(e_F \sin \omega_c + e_T \cos \omega_c, e_F \cos \omega_c - e_T \sin \omega_c) \\ \theta_2 = \theta_1 + \Delta\theta \end{cases} \quad (6)$$

where ω_c is the angle between the radius vector \mathbf{r}_1 and the chord unit vector \mathbf{i}_c , as shown in Fig. 1, and $\tan^{-1}(y, x)$ is the four-quadrant inverse tangent function. Then the exocentric anomaly can be calculated by the relationship between true and exocentric anomaly as follows:

$$E = 2 \tan^{-1} \left(\sqrt{\frac{1-e}{1+e}} \tan \frac{\theta}{2} \right) \quad (7)$$

From Eqs. (1–7), one can see that given the radius vectors \mathbf{r}_1 and \mathbf{r}_2 , the exocentric anomalies E_1 and E_2 , the semimajor axis, and the eccentricity of the transfer orbit can be expressed as a function of the transverse eccentricity e_T . With the help of E_1 , E_2 , a , and e , it is convenient to obtain the direct-transfer time t_{12}^s between P_1 and P_2 . The formulation of t_{12}^s , which is also a function of e_T , can be expressed as

$$t_{12}^s = \sqrt{\frac{a^3}{\mu}} [E_2 - E_1 - e(\sin E_2 - \sin E_1)] = f(\mathbf{r}_1, \mathbf{r}_2, e_T) \quad (8)$$

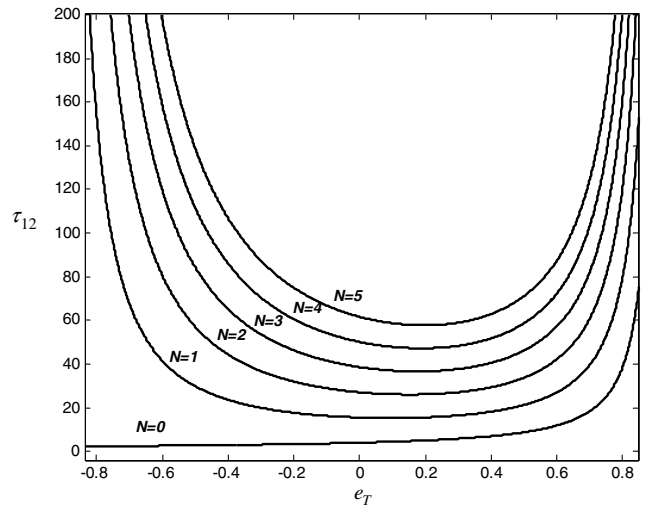
where $f(*)$ is defined as the direct-transfer-time function for the flight between P_1 and P_2 , which is similar to Avanzini's [1] formulation, considering the direct transfer only.

By adding multiples of the transfer orbit period to the direct-transfer time, Avanzini's formulation can now be generalized to the multiple-revolution case, which can be expressed as

$$t_{12} = N \cdot T(e_T) + f(\mathbf{r}_1, \mathbf{r}_2, e_T) = g(\mathbf{r}_1, \mathbf{r}_2, e_T, N) \quad (9)$$

where t_{12} is the multiple-revolution transfer time, N is the number of admissible revolutions, and $g(*)$ is defined as the extended transfer-time function. Thus, given two radius vectors \mathbf{r}_1 and \mathbf{r}_2 , the transfer time of the orbit is a function of N and e_T . Then the derivative of the transfer time with respect to the transverse eccentricity, dt_{12}/de_T , is derived, as shown in the Appendix. This derivative is needed for the Newton–Raphson iterative algorithm to solve the multiple-revolution problem in the next section. Moreover, multiple-revolution solutions are obtained for elliptic orbits only, so that the variation of the transverse eccentricity must be limited to the interval $-e_p < e_T < e_p$, where $e_p = \sqrt{1 - e_c^2}$.

In the following, the new multiple-revolution formulation is analyzed using canonical units. Following the approach in [1], distances are scaled with respect to r_1 , whereas time is scaled with respect to the reference time $t_{\text{ref}} = \sqrt{r_1^3/\mu}$. That is, the reference orbit has the radius $r_1 = 1$ and the gravitational constant $\mu = 1$.

Fig. 2 Transfer time as a function of e_T .

Letting $\tau_{12} = t_{12}/t_{\text{ref}}$, $\bar{\mathbf{r}}_1 = \mathbf{r}_1/r_1$, and $\bar{\mathbf{r}}_2 = \mathbf{r}_2/r_1$, the nondimensional transfer time is given by

$$\tau_{12} = g(\bar{\mathbf{r}}_1, \bar{\mathbf{r}}_2, e_T, N) \quad (10)$$

Figure 2 shows a multiple-revolution example plot of the nondimensional transfer time τ_{12} vs the transverse eccentricity e_T in the cases of different revolutions N , corresponding to the boundary conditions $r_2 = 2r_1$, and $\Delta\theta = 120^\circ$. For the case $N = 0$, the time τ_{12} is monotonically increasing with the transverse eccentricity e_T , which is the same as the analysis in [1] for the direct-transfer case. However, for each $N \geq 1$, the solutions do not vary monotonically, whereas there are, in general, two transverse eccentricities for a specified nondimensional desired transfer time τ_{12}^{des} , which correspond to a short-path and a long-path transfer orbit. Moreover, there is only one solution for e_T corresponding to the minimum flight time when the derivative dt_{12}/de_T equals zero. Following the conclusions of Prussing [5] and Shen and Tsotras [6], for the given τ_{12}^{des} , there are $2N_{\text{max}} + 1$ solutions for the multiple-revolution Lambert problem, where N_{max} is the maximum number of allowed revolutions.

III. Solutions of Multiple Revolution

In this section, a numerical procedure is presented to search the $2N_{\text{max}} + 1$ solutions for e_T , corresponding to the specified transfer time τ_{12}^{des} for the multiple-revolution Lambert problem. To provide a fast convergence rate, a coordinate transformation $x = \xi(e_T)$ is given, which is similar to that adopted in [1]. As mentioned above, because the elliptic orbit is the only conical orbit that affords multiple-revolution solutions [5], the admissible value of e_T is limited to the interval $-e_p < e_T < e_p$. Thus, a suitable transformation law is

$$x = \xi(e_T) = \frac{e_p}{2} \log \left(\frac{e_p + e_T}{e_p - e_T} \right) \quad (11)$$

As can be seen from Eq. (11), the value of x goes toward $-\infty$ when $e_T \rightarrow -e_p$, whereas it approaches $+\infty$ when $e_T \rightarrow +e_p$. Moreover, if e_T equals zero, x is equal to zero. The inverse transformation is thus given by

$$e_T = \xi^{-1}(x) = e_p \left[\exp \left(\frac{2x}{e_p} \right) - 1 \right] / \left[\exp \left(\frac{2x}{e_p} \right) + 1 \right] \quad (12)$$

Let y denote the logarithm of the nondimensional transfer time as follows:

$$y = \log(\tau_{12}) \quad (13)$$

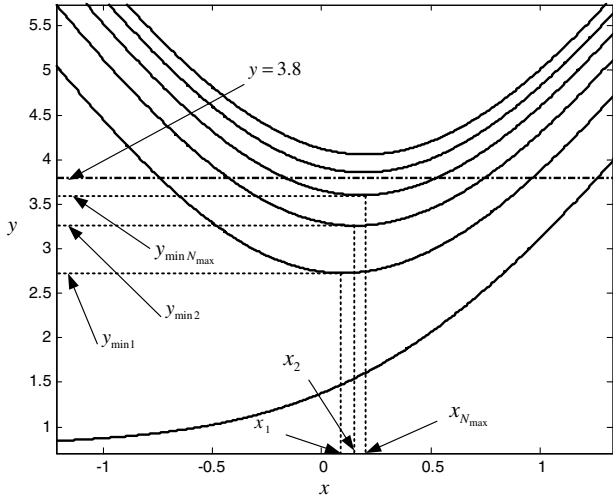


Fig. 3 Nondimensional transfer time as a function of x .

Then the derivative of y with respect to the transformed variable x is obtained by means of the chain rule as

$$\frac{dy}{dx} = \frac{1}{\tau_{12}} \cdot \frac{1}{t_{\text{ref}}} \cdot \frac{dt_{12}}{de_T} \cdot \frac{de_T}{dx} \quad (14)$$

where the derivation of dt_{12}/de_T is derived in the Appendix, and de_T/dx can be obtained from Eq. (12) as

$$\frac{de_T}{dx} = 4 \left/ \left[\exp\left(\frac{x}{e_p}\right) + \exp\left(-\frac{x}{e_p}\right) \right] \right|^2 \quad (15)$$

Figure 3 shows the plot of the transformed transfer time y vs the transformed variable x , which corresponds to the same boundary conditions used for deriving the results reported in Fig. 2.

The numerical algorithm to search the solutions of the multiple-revolution Lambert problem can be described with reference to the example reported in Fig. 3. For the specified radius vectors \bar{r}_1 and \bar{r}_2 and the transformed transfer time y_0 , the solutions are the points at which the curve $y = \log(\tau_{12})$ intersects the line $y = y_0$. The original problem is thus solved by finding all the solutions of an equation in the form

$$\log(\tau_{12}) - y_0 = 0 \quad (16)$$

The procedure is split into five steps:

- 1) Letting $N = 0$, calculate the root x_0 for Eq. (16) by Newton–Raphson iteration, using the derivative dy/dx [see Eq. (14)].
- 2) Letting $N = N + 1$, calculate the minimum values of the transformed transfer time $y_{\min N}$ at a particular value of x_N , when the derivative dy/dx equals zero.

3) Compare the value of y_0 with $y_{\min N}$. If $y_{\min N} \leq y_0$, go to step 4, whereas if $y_{\min N} > y_0$, go to step 5.

4) Calculate the two roots x_N^1 and x_N^2 for Eq. (16) (if $y_{\min N} = y_0$, $x_N^1 = x_N^2$), corresponding to the N -revolution Lambert problem by Newton–Raphson iteration using dy/dx , then go back to step 2.

5) Denote the maximum admissible number of revolutions as $N_{\max} = N - 1$, and the transverse eccentricity e_T corresponding to each root can be obtained using Eq. (12). In this way, all the multiple-revolution transfer orbits passing through P_1 and P_2 are determined.

Remark: This numerical procedure for searching solutions of the multiple-revolution Lambert problem is similar to the approach mentioned in [5,8], where it was used to solve the Lagrange formulation and universal-variable-based Lambert problem, respectively. Moreover, the convergence criterion for stopping the iterative process complies with the in equation $|y_0 - \log(\tau_{12})| < \varepsilon$, with the specified tolerance $\varepsilon = 10^{-12}$. The initial guess for the solution x_0 in step 1) is $x_{N_0} = 0$ when $N = 0$, whereas the initial guesses for the solutions x_N^1 and x_N^2 in step 4) are $x_{N_0}^1 = x_N - 1$ and $x_{N_0}^2 = x_N + 1$ when $N \geq 1$.

IV. Numerical Examples

Some numerical examples solved by means of the approach outlined in the previous section are now discussed to demonstrate the new method and assess its performance. Table 1 reports the results obtained in four different cases, labeled in the first column from 1 to 4, which differs in terms of ratios of the transfer radii r_2/r_1 and values of the transfer angle. Case 1 corresponds to the conditions $r_2 = 2r_1$, and $\Delta\theta = 60^\circ$; in case 2, it is $r_2 = 0.5r_1$, and $\Delta\theta = 120^\circ$; case 3 assumes $r_2 = 1.5r_1$, and $\Delta\theta = 180^\circ$; and, case 4 considers a large transfer angle, $\Delta\theta = 240^\circ$, with $r_2 = 2r_1$.

In Table 1, the second column gives the specified nondimensional desired transfer time τ_{12}^{des} , and the maximum number of the revolution allowed for each case is shown in column 3. The orbital speeds at point P_1 and P_2 during the transfer, calculated by the transverse-eccentricity-based method, are given in columns 4 and 5 in the unit of $v_{\text{ref}} = r_1/t_{\text{ref}}$, along with the corresponding number of revolutions N in the sixth column. Next, the variable L/S indicates whether the transfer orbit is the long- or short-path Lambert solution for each $N > 0$. The last six columns show the iteration numbers required for certain accuracy and the corresponding time cost required for 100,000 time calculations by three methods applied in the simulation on the same platform. The first two methods are both based on the transverse-eccentricity approach, and the third one is based on Bate et al.'s [7] work. Between the first two methods, the difference lies in the iterated functions used in the Newton–Raphson iteration. The former one adopts the derivative dy/dx in the iterated function, and the latter one uses Avanzini's [1] approach, in which the derivative is evaluated by the numerical difference method. Simulation shows that the first two methods based on the transverse eccentricity can give solutions of the orbital speeds in perfect accordance with Bate et al.'s

Table 1 Multiple solutions for four cases

Case	τ_{12}^{des}	N_{\max}	e_T method				Number of iterations			Time cost(s)		
			\bar{v}_1	\bar{v}_2	N	L/S	e_T	NDe_T	Bate et al. [7]	e_T	NDe_T	Bate et al. [7]
1	20	2	1.253258	0.755417	0	—	4	6	6	34.6	45.1	21.4
			1.227040	0.711074	1	L	4	6	5			
			1.152185	0.572303	1	S	4	6	7			
			1.087058	0.426256	2	L	5	8	7			
			1.074602	0.393407	2	S	5	8	8			
2	10	2	1.144571	1.819352	0	—	4	6	6	31.8	44.7	20.3
			1.102109	1.792943	1	L	4	6	6			
			0.957520	1.707877	1	S	4	5	6			
			0.849238	1.649608	2	L	5	7	7			
			0.784537	1.617250	2	S	5	7	7			
3	10	0	1.172585	0.841600	0	—	3	5	6	16.2	28.3	11.9
4	20	1	1.255690	0.759445	0	—	3	5	7	25.5	39.1	17.6
			1.217259	0.694061	1	L	4	6	6			
			1.160670	0.589198	1	S	4	6	7			

[7] algorithm, but less efficient because they require a higher computational cost to implement a single iteration. However, the first method, with the analytical derivative dy/dx adopted, outdoes the second one using the NDe_T method by saving 31.2% of computing time on average.

V. Conclusions

The main objective of this Note is to extend the solution method for the Lambert problem based on the transverse eccentricity to the case of multiple-revolution transfers, presenting an explicit formulation for the derivative of the transfer time with respect to the transverse eccentricity. Using the analytical derivative, the multiple-revolution solutions can be obtained more efficiently than by means of the numerical difference originally adopted for the transverse-eccentricity method. Though the transverse-eccentricity-based algorithm seems less efficient in comparison with the classical one, it provides a new way to solve the Lambert problem, based on classical orbit elements.

Appendix

In this Appendix, the derivation of dt_{12}/de_T needed for the Newton–Raphson iterative algorithm is derived, starting from Eq. (9) as

$$t_{12} = N \cdot T(e_T) + f(\mathbf{r}_1, \mathbf{r}_2, e_T) \quad (\text{A1})$$

Taking the derivative with respect to the transverse eccentricity e_T , the expression for dt_{12}/de_T is given by

$$\frac{dt_{12}}{de_T} = N \frac{\partial T}{\partial a} \cdot \frac{da}{de_T} + \frac{\partial f}{\partial a} \cdot \frac{da}{de_T} + \frac{\partial f}{\partial e} \cdot \frac{de}{de_T} + \frac{\partial f}{\partial E_1} \cdot \frac{dE_1}{de_T} + \frac{\partial f}{\partial E_2} \cdot \frac{dE_2}{de_T} \quad (\text{A2})$$

From Eqs. (4) and (5), the partial derivative $\partial T/\partial a$ is

$$\frac{\partial T}{\partial a} = 3\pi \sqrt{\frac{a}{\mu}} \quad (\text{A3})$$

and the derivative da/de_T is

$$\frac{da}{de_T} = \frac{\partial a}{\partial p} \cdot \frac{dp}{de_T} + \frac{\partial a}{\partial e_T} \cdot \frac{de_T}{de_T} = \frac{\partial a}{\partial p} \cdot \frac{dp}{de_T} + \frac{\partial a}{\partial e_T} \quad (\text{A4})$$

where

$$\frac{\partial a}{\partial p} = \frac{1}{1 - e^2} \quad (\text{A5})$$

$$\frac{dp}{de_T} = -\frac{r_1 r_2}{c} \sin \Delta \theta \quad (\text{A6})$$

$$\frac{\partial a}{\partial e_T} = \frac{2p \cdot e_T}{(1 - e^2)^2} = \frac{2a \cdot e_T}{(1 - e^2)} \quad (\text{A7})$$

From Eq. (8), the corresponding partial derivatives are

$$\frac{\partial f}{\partial a} = \frac{3}{2} \sqrt{\frac{a}{\mu}} [E_2 - E_1 - e(\sin E_2 - \sin E_1)] \quad (\text{A8})$$

$$\frac{\partial f}{\partial e} = \sqrt{\frac{a^3}{\mu}} (\sin E_1 - \sin E_2) \quad (\text{A9})$$

$$\frac{\partial f}{\partial E_1} = \sqrt{\frac{a^3}{\mu}} (\cos E_1 - 1) \quad (\text{A10})$$

and

$$\frac{\partial f}{\partial E_2} = \sqrt{\frac{a^3}{\mu}} (1 - \cos E_2) \quad (\text{A11})$$

It is easy to get the derivative de/de_T by

$$\frac{de}{de_T} = \frac{e_T}{e} \quad (\text{A12})$$

and the derivative dE_1/de_T can be obtained from Eqs. (6) and (7) as follows:

$$\frac{dE_1}{de_T} = \frac{\partial E_1}{\partial \theta_1} \cdot \frac{d\theta_1}{de_T} + \frac{\partial E_1}{\partial e} \cdot \frac{de}{de_T} \quad (\text{A13})$$

where

$$\frac{\partial E_1}{\partial \theta_1} = \frac{\sqrt{1 - e^2}}{1 + e \cos \theta_1} \quad (\text{A14})$$

$$\frac{d\theta_1}{de_T} = -\left(\arctan \left(\frac{e_F \sin \omega_c + e_T \cos \omega_c}{e_F \cos \omega_c - e_T \sin \omega_c} \right) \right)' = -\frac{e_F}{e^2} \quad (\text{A15})$$

and

$$\frac{\partial E_1}{\partial e} = \frac{-\sin \theta_1}{1 + e \cos \theta_1} \cdot \frac{1}{\sqrt{1 - e^2}} \quad (\text{A16})$$

The expression for dE_2/de_T can be obtained similarly.

Acknowledgments

This work was supported by the National Basic Research Program of China (grant no. 2009CB723900). The authors would also like to thank all the anonymous reviewers and editors for their valuable comments and suggestions.

References

- [1] Avanzini, G., "A Simple Lambert Algorithm," *Journal of Guidance, Control, and Dynamics*, Vol. 31, No. 6, 2008, pp. 1587–1594. doi:10.2514/1.36426
- [2] Battin, R. H., "Lambert's Problem Revisited," *AIAA Journal*, Vol. 15, No. 5, 1977, pp. 707–713. doi:10.2514/3.60680
- [3] Battin, R. H., *An Introduction to the Mathematics and Methods of Astrodynamics*, AIAA Education Series, AIAA, New York, 1987, Chaps. 6–7.
- [4] Ochoa, S. I., "Multiple Revolution Solutions to Lambert's Problem," M.S. Thesis, Dept. of Aeronautical and Astronautical Engineering, Univ. of Illinois at Urbana–Champaign, Urbana, IL, 1991.
- [5] Prussing, J. E., "A Class of Optimal Two-Impulse Rendezvous Using Multiple-Revolution Lambert Solutions," *Journal of the Astronautical Sciences*, Vol. 48, Nos. 2–3, April–Sept. 2000, pp. 131–148; also American Astronautical Society Paper AAS 00-250.
- [6] Shen, H. J., and Tsionas, P., "Optimal Two-Impulse Rendezvous Using Multiple-Revolution Lambert Solutions," *Journal of Guidance, Control, and Dynamics*, Vol. 26, No. 1, 2003, pp. 50–61. doi:10.2514/2.5014
- [7] Bate, R. R., Mueller, D. D., and White, J. E., *Fundamentals of Astrodynamics*, Dover, New York, 1971, pp. 227–276.
- [8] Han, C., and Xie, H. W., "Research on Algorithm of Loopy Lambert Transfer in Space Rendezvous," *Chinese Space Science and Technology*, Vol. 24, No. 5, 2004, pp. 9–14.